RESEARCH ARTICLE OPEN ACCESS

Amauroderma rugosum Extract Improves Brain Function in D-Galactose-Induced Aging Mouse Models via the Regulatory Effects of Its Polysaccharides on Oxidation, the mTOR-Dependent Pathway, and Gut Microbiota

Panthakarn Rangsinth[1] (ID) | Chengwen Zheng[1] | Polly Ho-Ting Shiu[1] | Wen Wang[1] | Tsz Ching Kwong[2] | Chi Tung Choy[3] | Susan Wai-Sum Leung[1] | Tewin Tencomnao[4] | Siriporn Chuchawankul[5] | Anchalee Prasansuklab[6] | Timothy Man-Yau Cheung[7] | Yiu-Wa Kwan[2] | Priya Kannan[8] | Jingjing Li[8] | George Pak-Heng Leung[1] (ID)

[1]Department of Pharmacology and Pharmacy, The University of Hong Kong, Hong Kong SAR, China | [2]School of Biomedical Sciences, The Chinese University of Hong Kong, Hong Kong, China | [3]Microbiome Research Centre, BioMed Laboratory Company Limited, Hong Kong, China | [4]Department of Clinical Chemistry, Faculty of Allied Health Sciences, Chulalongkorn University, Bangkok, Thailand | [5]Department of Transfusion Medicine and Clinical Microbiology, Faculty of Allied Health Sciences, Chulalongkorn University, Bangkok, Thailand | [6]College of Public Health Sciences, Chulalongkorn University, Bangkok, Thailand | [7]Tian Ran Healthcare Limited, Hong Kong, China | [8]Department of Rehabilitation Sciences, Faculty of Health and Social Sciences, Hong Kong Polytechnic University, Hong Kong SAR, China

Correspondence: Jingjing Li (kim07.li@polyu.edu.hk) | George Pak-Heng Leung (gphleung@hku.hk)

ABSTRACT

The pharmacological effects of *Amauroderma rugosum* (AR), an edible mushroom found mainly in Southeast Asia, are not well studied, particularly its neuroprotective properties. This study investigated the neuroprotective effects of AR aqueous extract (ARW) in a D-galactose-induced accelerated aging mouse model and senescent SH-SY5Y neuronal cells. Behavioral tests (open field, Morris water maze, Y-maze, and rotarod) demonstrated that D-galactose-induced aging mice exhibited impaired cognitive function, memory loss, anxiety, and reduced locomotor ability, all of which were alleviated by ARW treatment. Histological analysis showed that ARW reduced neuropathological lesions in the hippocampus. In SH-SY5Y neuronal cells, ARW and AR polysaccharide extract (ARP) enhanced cell viability and decreased intracellular reactive oxygen species (ROS) levels in a concentration-dependent manner. ARW and ARP also reduced cellular senescence and apoptosis in D-galactose-treated cells. Western blot analysis indicated that ARW and ARP upregulated the phosphorylation of mTOR and increased the expression of antioxidant enzymes, including superoxide dismutase 1 and heme-oxygenase-1. Additionally, ARW altered the gut microbiota, increasing the relative abundance of beneficial bacteria such as *Lactobacillus reuteri* and decreasing harmful bacteria like *Clostridium scindens*. These findings suggest that AR exerts neuroprotective effects primarily through its polysaccharides by modulating oxidative stress, activating the mTOR-dependent pathway, and influencing the gut microbiota. Consequently, AR could serve as a potential dietary supplement for the prevention and treatment of neurodegenerative diseases.

1 | Introduction

Aging is a natural yet intricate process characterized by gradual alterations in multiple physiological functions and the onset of various chronic illnesses. Brain aging is key because of its prominent role in impairing the nervous system through memory decline, amnesia, cognitive disorders, and dementia, which can significantly hinder normal functioning. Donepezil, rivastigmine, galantamine, and memantine are widely prescribed for the treatment of Alzheimer's disease (AD). However, prolonged high-dose treatment may lead to adverse effects (Kose et al. 2023). Therefore, there is an urgent need to develop new drugs to prevent and treat neurodegenerative diseases.

Neurons cannot undergo cell division; therefore, neuronal death is permanent, and the changes that occur in neurons due to aging cannot be reversed. Oxidative stress, a condition characterized by an imbalance between the production of reactive oxygen species (ROS) and the ability of cells to detoxify them, is increased in brain cells due to aging. This phenomenon has been recognized as a crucial factor in the progression of age-related neurodegenerative diseases (Goldsteins et al. 2022). Thus, improving the brain's ability to counteract oxidative stress may be a logical approach to preserving optimal function during aging. Several natural products, such as vitamin A, vitamin C, vitamin E, polyphenols, and carotenoids, have been recommended for the management of age-related diseases because of their antioxidant properties, which either directly neutralize free radicals or improve the performance of antioxidant enzymes (Mani et al. 2023).

Amauroderma rugosum (AR), a group of basidiomycetes, belongs to the Ganodermataceae family. Its geographical distribution encompasses China, the South Pacific, the South Atlantic, Indonesia, Taiwan, Equatorial Guinea, and Australia and is predominantly cultivated in tropical and subtropical climates. The appearance of AR is unique. The cap of the AR fruiting body exhibits a color gradient from taupe to black, featuring either blunt or thin edges, a tomentose texture, and irregular wrinkles. The surface of the AR gills is white, but it becomes dark red upon scratching. Therefore, AR is also called "Blood Lingzhi" in Chinese due to its "bleeding" properties when scratched. AR is utilized in traditional Chinese medicine to treat acute and chronic nephritis and dyspepsia. Although limited pharmacological studies exist on AR, it possesses antioxidant, anti-inflammatory, anti-cancer, anti-hyperlipidemic, anti-epileptic, gastric protective, and antimicrobial properties (Zheng, Cheung, and Leung 2022). Interestingly, the antioxidant effect of AR surpasses that of other extensively researched mushrooms in the Ganodermataceae family, including *Ganoderma lucidum* and *Ganoderma sinense* (Xiao, Liu, and He 2017; Zheng, Cheung, and Leung 2022). The remarkable antioxidant properties of AR may render it beneficial for the treatment and prevention of age-related issues, including neurodegenerative diseases. Our previous study has shown that AR aqueous extract (ARW) protects PC12 and SH-SY5Y neuronal cells from oxidative stress, mitochondrial dysfunction, and apoptosis triggered by 6-hydroxydopamine (Li et al. 2021; Rangsinth et al. 2024). However, the neuroprotective efficacy of AR has not yet been substantiated in animal models.

Hence, this study used a D-galactose-induced aging mouse model to investigate the neuroprotective effects of AR in vivo. D-Galactose-induced senescence in SH-SY5Y cells was used to examine the effects of AR on oxidative stress, mitochondrial function, and apoptosis. The effect of AR on the intestinal flora, which may indirectly affect brain function through the microbiota–gut–brain axis, was also explored, along with the active ingredients and mechanisms underlying the neuroprotective effects of AR.

2 | Materials and Methods

2.1 | Materials

The fruiting bodies of AR were provided by Tian Ran Healthcare Ltd. (Hong Kong, China). Dulbecco's modified Eagle's medium (DMEM), fetal bovine serum (FBS), 4′,6-diamidino-2-phenylindole (DAPI), penicillin–streptomycin, and 0.25% (w/v) trypsin containing 1 mM ethylenediaminetetraacetic acid, CM-H_2DCFDA, 5,5′,6,6′-tetrachloro-1,1′,3,3′-tetraethylbenzimidazolocarbocyanine iodide (JC-1), Annexin V-conjugated fluorescein isothiocyanate (FITC), and propidium iodide (PI) were purchased from Invitrogen (Carlsbad, CA, USA). The bicinchoninic acid assay kit was acquired from Boster Biological Technology Co. Ltd. (Pleasanton, CA, USA). All the antibodies used for western blotting were purchased from Cell Signaling Technology (Danvers, MA, USA). All other chemicals were purchased from Sigma-Aldrich (St. Louis, MO, USA).

2.2 | Preparation of Water Extracts of ARW and *Amauroderma rugosum* Polysaccharides (ARP)

The samples were dried and ground into powder. A reflux system was used to prepare the ARW. Two grams of the powder were extracted with 50 mL of distilled water at 95°C $\pm$ 2°C for 60 min. The crude extract was centrifuged at 4000 $\times$ *g* for 20 min. The supernatant was collected, and the sample residue was re-extracted twice using the abovementioned steps. Subsequently, all extracts were pooled, filtered, and concentrated to 80 mL using a rotary evaporator. ARP was prepared from ARW via ethanol precipitation, with a final ethanol percentage of 80. The ARP was lyophilized using a freeze-dryer. ARW and ARP were stored at −20°C until further use. The extracts were diluted to suitable concentrations and filtered through membrane filters with a pore size of 0.22 μm before experiments.

2.3 | Measurement of Polysaccharide, Triterpene, Total Phenolic Compound, and Protein Content

The amounts of polysaccharides, triterpenes, and total phenolic compounds were quantified by phenol-sulfuric acid, vanillin-perchloric acid, and the Folin–Ciocalteu method, respectively (Li et al. 2021). The standards used for the chemical analysis of polysaccharides, phenolic compounds, flavonoids, and triterpenes were glucose (GE), gallic acid (GAE), quercetin (QE), and oleanolic acid (OA), respectively.

2.4 | D-Galactose-Induced Accelerated-Aging Mouse Model

All animal experiments were approved by the Committee on the Use of Live Animals in Teaching and Research of the University of Hong Kong (protocol number: 6038-22). C57/BL6J mice (8 weeks old, both male and female) were supplied by the Center for Comparative Medicine Research of the University of Hong Kong. The mice were kept in disinfected cages in a temperature-controlled room (16°C–26°C) with a 12 h light/dark cycle and had free access to distilled water and standard diet chow. After a 7-day adaptation period, the mice were randomly divided into five groups: (1) control ($n = 10$), (2) D-galactose ($n = 10$), (3) D-galactose with 50 mg/kg ARW ($n = 10$), (4) D-galactose with 100 mg/kg ARW ($n = 10$), and (5) D-galactose with 50 mg/kg vitamin C ($n = 10$). Equal numbers of male and female mice were assigned to each treatment group. Aging was induced by intraperitoneal injection of 200 mg/kg of D-galactose daily for 12 weeks, whereas mice in the control group were injected with 0.9% saline. During the 12 weeks, ARW and vitamin C were administered daily by oral gavage. Vitamin C served as a positive control in this study because of its capacity to diminish oxidative stress, inflammation, senescence, and the development of protein spongiosis and tangles in brain cells (Lin et al. 2021; Nam et al. 2019; Reshma et al. 2022). Besides, the oral administration of vitamin C inhibits D-galactose-induced impairment of hippocampal neurogenesis by enhancing cellular proliferation, neuronal differentiation, and neuronal maturation (Nam et al. 2019). Vitamin C also restores the expression of synaptic plasticity-related markers in D-galactose-treated mice brains (Nam et al. 2019). Additionally, vitamin C enhances locomotor activities in D-galactose-treated mice, as evidenced by the open field and rotarod tests (Reshma et al. 2022), and improves memory function in the novel location recognition test (Nam et al. 2019).

2.5 | Open Field Test

The mice were subjected to an open field test to estimate their locomotion and anxiety-like behavior. Individual mice were allowed to move freely in an open field box (length, 40 cm; width, 40 cm; height, 40 cm) for 10 min. An area of 20×20 cm^2 in the middle was defined as the center zone, and the rest was defined as the corner zone. Videos were recorded to monitor the movement of the mice. Data on the total distance moved, speed, and time spent in the center zone of the field were analyzed using the SMART video tracking software (version 3.0; Panlab S.L.U., Barcelona, Spain).

2.6 | Morris Water Maze Test

The Morris water maze test was used to assess memory and cognitive functions. Briefly, mice were trained to find a hidden circular platform (10 cm) in a pool (120 cm in diameter) with distal cues on the pool wall. The pool was filled with tap water mixed with non-toxic white paint. Each mouse underwent three acquisition trials daily for 5 days of cued training. During the training step, mice were introduced into the water near the edge of the pool facing the wall. They were then placed on a submerged

platform for 1 min. They were guided gently if they failed to find the platform within 1 min. The mice stayed on the platform for 10 s and then were taken from the pool. The mice repeated the trial with at least a 1 h interval between each repetition. Although the start position was changed with every trial, the location of the platform remained stationary. Acquisition testing was initiated on Day 6. The platform was removed from the pool, and the mice were introduced into the water from a novel entry point. The mice were allowed to swim freely for 1 min, and the SMART video tracking software was used to track and analyze escape latency, quadrant preference, and swimming speed.

2.7 | Y-Maze Test

The Y-maze test was used to assess spatial working memory and employed a Y-maze apparatus (length: 30 cm; width: 8 cm per arm). In the training session, one arm was closed and assigned as a hidden arm, and two open arms were freely accessed. Individual mice were placed facing the center in one of the open arms and allowed to move freely (12-min sessions). After a 1-h interval, the hidden arm was opened. During the test run, the mice were placed in the same arm and allowed to explore the maze freely for 5 min. Videos were recorded and analyzed using the SMART video tracking software.

2.8 | Rotarod Test

The rotarod test was used to evaluate motor skill learning and coordination. The mice were trained to familiarize themselves with the rotarod (Panlab, Harvard Apparatus, MA, USA) at 5 rotations per minute (rpm) for at least 1 min. If the mice failed to remain on the rotating rod for less than 1 min, training was restarted until they remained on the rotating rod for 1 min without falling. Five minutes after the training session, they were tested on a rotating rod with an auto-accelerating speed ranging from 4 to 40 rpm over 300 s. The latency and rotating speed required to maintain balance on the rotarod for each mouse were recorded across three trials at 5-min intervals.

2.9 | Histological Examination of Tissue Morphology

Brain tissues were fixed in 4% formaldehyde, embedded in paraffin, sectioned (4-µm slices), and stained with hematoxylin and eosin. Hippocampal morphology was examined under a microscope.

2.10 | Fecal Sample Collection and 16S rRNA Sequencing

Fecal samples were collected from the mice and promptly stored in 2 mL of preservation buffer at 4°C. Microbial genomic DNA was extracted using a QIAamp PowerFecal Pro DNA Kit (Qiagen, Hilden, Germany). The 16S rRNA sequences were analyzed as previously described (Kwong et al. 2023). Briefly, a Nextera XT DNA Library Preparation Kit was used to amplify the V3–V4 region of the 16S rRNA gene. Paired-end sequencing was

performed on the NovaSeq platform (Illumina, San Diego, CA, USA) using Novogene (Hong Kong, China). Before downstream analysis, index barcodes and adapter sequences were trimmed from paired-end demultiplexed reads.

2.11 | Sequencing Data and Bioinformatics Analysis

Sequencing data were analyzed using the Quantitative Insights into Microbial Ecology (QIIME) 2-2023.2. Demultiplexed reads were quality-controlled and denoised using DADA2 to retrieve exact amplicon sequence variants (ASVs). All ASVs were aligned using MAFFT, and a phylogenetic tree was generated using fastree2 via the q2-phylogeny plugin. Taxonomic annotation of the resulting ASV was conducted using the q2-feature-classifier plugin and a pre-trained Naïve Bayes classifier, which was based on the SILVA v138 taxonomic reference database with 99% similarity. The six metrics used to indicate α diversity were as follows: observed operational taxonomic units (OTUs), Chao1 Index (Chao1), ACE Index (ACE), Shannon Diversity Index (Shannon), Simpson Index (Simpson), and Faith's phylogenetic diversity (PD). In addition, β diversity was calculated on the basis of cosine, Hamming, Jaccard, Bray–Curtis, weighted UniFrac, and unweighted UniFrac distance metrics. The PERMANOVA test for β diversity was used to compare microbial community dissimilarities across groups. A differential abundance analysis was conducted using ANCOM with bias correction (ANCOM-BC).

2.12 | Cell Culture

Human neuroblastoma SH-SY5Y cells were obtained from the American Type Culture Collection (Manassas, VA, USA). The cells were cultured in DMEM supplemented with 10% FBS, 100 U/mL penicillin, and 100 µg/mL streptomycin and maintained at 37°C in a humidified atmosphere containing 5% CO_2. The cells were differentiated through 48-h incubation with 10 µM retinoic acid before conducting subsequent studies.

2.13 | Cell Viability Assay

Cell viability was measured using the MTT assay according to the manufacturer's protocol. Briefly, after drug treatment, the cell culture medium was replaced with an MTT solution (0.5 mg/mL), and the cells were incubated for an additional 3 h at 37°C. The MTT solution was discarded, and 100 µL of DMSO was added to each well to dissolve the violet formazan crystals formed within the cells. Absorbance at 560 nm was measured using a SpectraMax M5 Multi-Mode Microplate Reader (Molecular Devices, Sunnyvale, CA, USA).

2.14 | Measurement of Intracellular ROS

The cells were washed with phosphate-buffered saline (PBS) and stained with 2 µM CM-H2DCFDA at 37°C for 15 min. After washing with PBS to remove unbound dyes, the cells were detached from the culture plates using 0.25% trypsin. The cells were then resuspended and examined by flow cytometry (BD

Biosciences) to detect 10,000 cells in each sample. The data were analyzed using the FlowJo software (version 10.4).

2.15 | Assessment of Cell Apoptosis

Apoptosis was assessed using Annexin V/PI double staining. After drug treatment, the cells were washed twice with cold PBS. The cells were then suspended in the binding solution and stained with Annexin V-FITC and PI (1.0 mg/mL) for 20 min. The stained cells were promptly evaluated using flow cytometry, and 10,000 events were recorded for each sample. The data were analyzed using the FlowJo software.

2.16 | Assessment of the β-Galactosidase Level

The aging marker β-galactosidase was detected using a Senescence Assay Kit (Abcam), following the manufacturer's instructions. Briefly, the SH-SY5Y cells were washed with PBS, after which fresh media containing senescent dye was added. The cells were then incubated for 1 h at 37°C in an atmosphere of 5% CO_2. The SH-SY5Y cells were trypsinized and resuspended. The stained cells were promptly evaluated using flow cytometry, and 10,000 events were recorded for each sample. The data were analyzed using the FlowJo software.

2.17 | Western Blot Analysis

Proteins were extracted from the SH-SY5Y cells, and western blotting was carried out as described previously (Rangsinth et al. 2024). The membranes were probed with primary antibodies targeting mTOR, phospho-mTOR (Ser2448), Akt, phospho-Akt (Ser473), superoxide dismutase (SOD)-1, catalase (CAT), or heme-oxygenase (HO)-1. The optical density values for different bands of the blots were normalized to those of β-actin.

2.18 | Data and Statistical Analyses

Data are expressed as mean ± standard deviation (SD). Statistical analyses were performed using one-way ANOVA, followed by Tukey's multiple comparison tests (two or more groups) using the GraphPad Prism software (version 6.0; GraphPad Software Inc., San Diego, CA, USA). $p < 0.05$ was considered significant.

3 | Results

3.1 | Effects of the ARW on the Weights of the Body, Brain, Liver, and Spleen of Mice

As shown in Figure 1A and Table 1, the body weights of male and female mice in all groups increased by approximately 11 and 7 g, respectively, during the 12-week experimental period. No significant differences were observed among the control and treatment groups ($p > 0.05$), indicating that D-galactose, vitamin C, and ARW, at the doses used in the study, had no significant effects on the body weight of mice. Additionally, the weights of organs, including the brain, liver, and spleen, were measured after
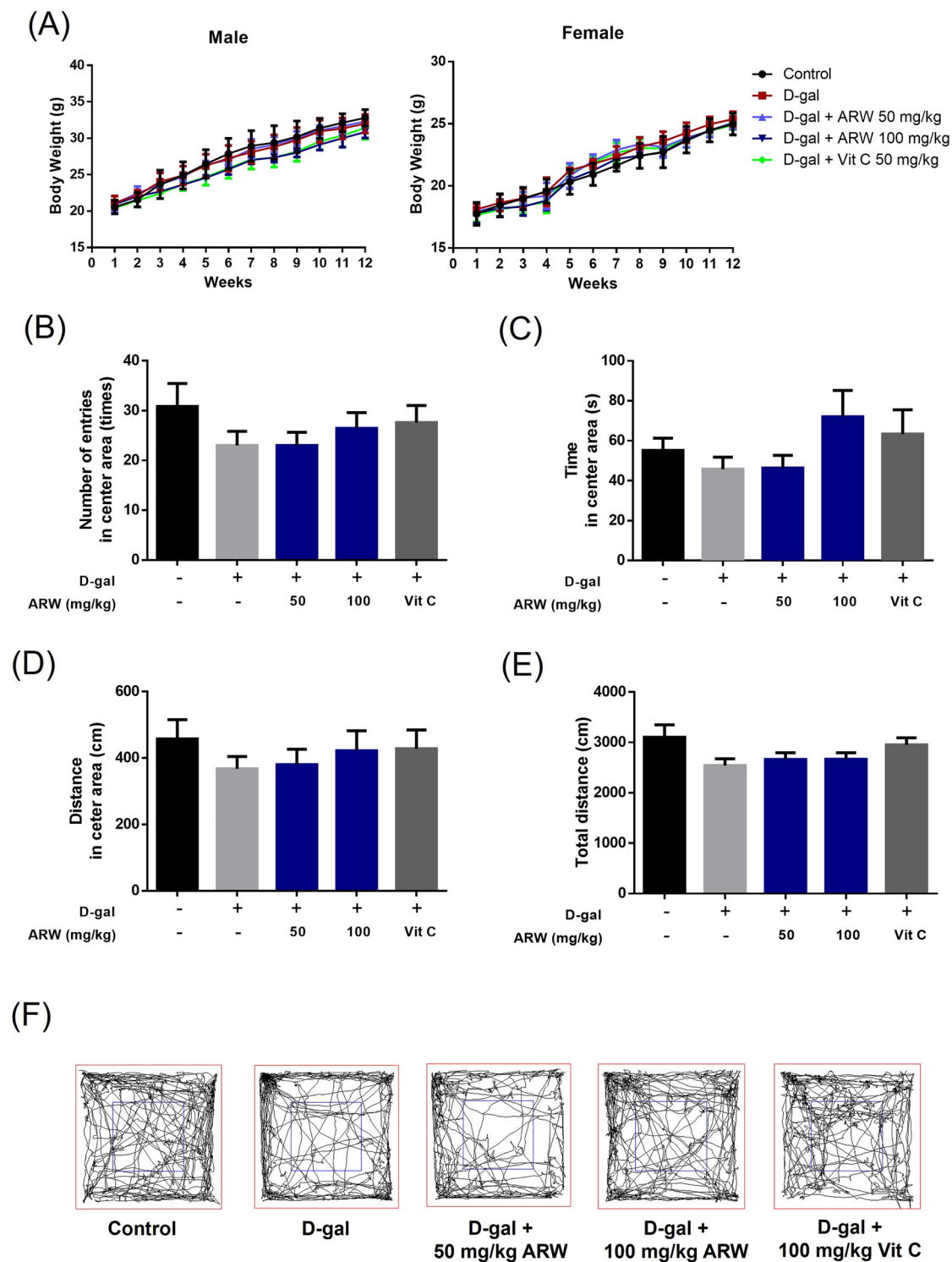
FIGURE 1 | **Effect of *Amauroderma rugosum* extract (ARW) treatment on body weight, general locomotor activity, anxiety, and willingness to explore in D-galactose-induced aging mice**. The mice were treated with D-galactose for 12 weeks with different doses of ARW. Mice that received no treatment were used as the control group. The vitamin C–treated group was used for comparison. An open field test was performed after treatment. (A) The body weight of the mice was recorded every week during the treatment period. (B) Number of entries in the center area, (C) time spent in the center area, (D) distance in the center area, (E) total distance traveled by the animal, and (F) the path of movement were measured for all experimental groups. Bars represent the mean ± standard deviation of 10 independent experiments.

TABLE 1 | Body, brain, liver, and spleen weights of mice after the 12-week treatment.

Group	Body (g)		Brain (g)		Liver (g)		Spleen (g)	
	Male	Female	Male	Female	Male	Female	Male	Female
Control	32.80 ± 1.13	24.98 ± 0.87	0.481 ± 0.050	0.472 ± 0.040	1.356 ± 0.282	1.017 ± 0.185	0.081 ± 0.008	0.081 ± 0.014
D-gal	32.00 ± 1.27	25.38 ± 0.51	0.492 ± 0.059	0.477 ± 0.014	1.373 ± 0.210	1.126 ± 0.169	0.084 ± 0.038	0.081 ± 0.012
D-gal + 50 mg/kg ARW	32.30 ± 0.66	25.03 ± 0.40	0.471 ± 0.063	0.453 ± 0.054	1.353 ± 0.237	1.056 ± 0.203	0.085 ± 0.012	0.080 ± 0.021
D-gal + 100 mg/kg ARW	30.87 ± 0.81	25.07 ± 0.47	0.450 ± 0.058	0.422 ± 0.068	1.322 ± 0.135	1.031 ± 0.136	0.084 ± 0.027	0.080 ± 0.009
D-gal + 50 mg/kg vitamin C	31.43 ± 1.57	24.90 ± 0.36	0.486 ± 0.004	0.450 ± 0.022	1.252 ± 0.097	1.105 ± 0.061	0.084 ± 0.014	0.082 ± 0.012

Abbreviation: ARW, *Amauroderma rugosum* extract.

the mice were sacrificed, and no statistical differences were found among the groups ($p > 0.05$; Table 1). The weights of the liver and spleen serve as indicators of drug toxicity, and on the basis of the findings, ARW was proven to be non-toxic.

3.2 | Effects of the ARW on General Locomotor Activity Levels, Anxiety, and Willingness to Explore in Aging Mice

The results of the open field test showed that the D-galactose-induced aging mice spent less time in the central area of the open field box when compared to the mice in the control group (from 55.17 to 45.80 s) (Figure 1C). However, after treatment with the ARW (100 mg/kg), the mice with D-galactose-induced accelerated aging were more willing to walk and explore the central area (72.06 s; Figure 1C). Although a statistically significant difference could not be achieved, this trend suggests that the ARW may enhance locomotor activity and reduce anxiety during aging. Further, there was no difference between the male and female mice (Figure S1).

## 3.3 | Effects of ARW on Memory and Cognitive Function in Aging Mice

As reflected by the number of platform crossings (Figure 2D), latency in the platform zone and platform quadrant (Figure 2E,F), and distance traveled in the platform zone and target quadrant (Figure 2G,H) in the Morris water maze test, D-galactose-induced aging mice apparently spent less time in the platform zone, indicating impaired memory and cognitive functions. Although a statistically significant difference could not be reached, there was a trend that the above parameters were improved when the mice were treated with the ARW (Figure 2D–G). Specifically, the latency in the platform zone decreased from 2.28 to 1.32 s after the mice were treated with D-galactose (Figure 2E), whereas the time was increased to 2.98 s after treatment with 100 mg/kg ARW. In addition, the D-galactose-induced aging mice traveled at a slower speed, decreasing from 18.75 to 15.16 cm/s (Figure 2B), indicating that their locomotor function was also reduced. The speed increased to 16.80 cm/s after treatment with 100 mg/kg ARW. There was no difference between the male and female mice (Figure S2).

3.4 | Effect of the ARW on the Spatial Reference Memory Function in Aging Mice

The results of the Y-maze test showed that the number of novel arm entries, distance traveled, and time spent in the novel arm were significantly lower than in the control group (Figure 3). However, after treatment with 100 mg/kg ARW, D-galactose-induced aging mice traveled longer and spent more time in the novel arm (Figure 3B,C). Specifically, the average distance in the novel arm decreased from 362.83 to 249.60 cm when the mice were treated with D-galactose but increased to 394.00 cm when the aging mice were simultaneously treated with 100 mg/kg ARW. Similarly, the time spent in the novel arm decreased from 101.26 to 51.61 s after treatment with D-galactose. However, the time increased to 107.96 s when D-galactose-treated mice
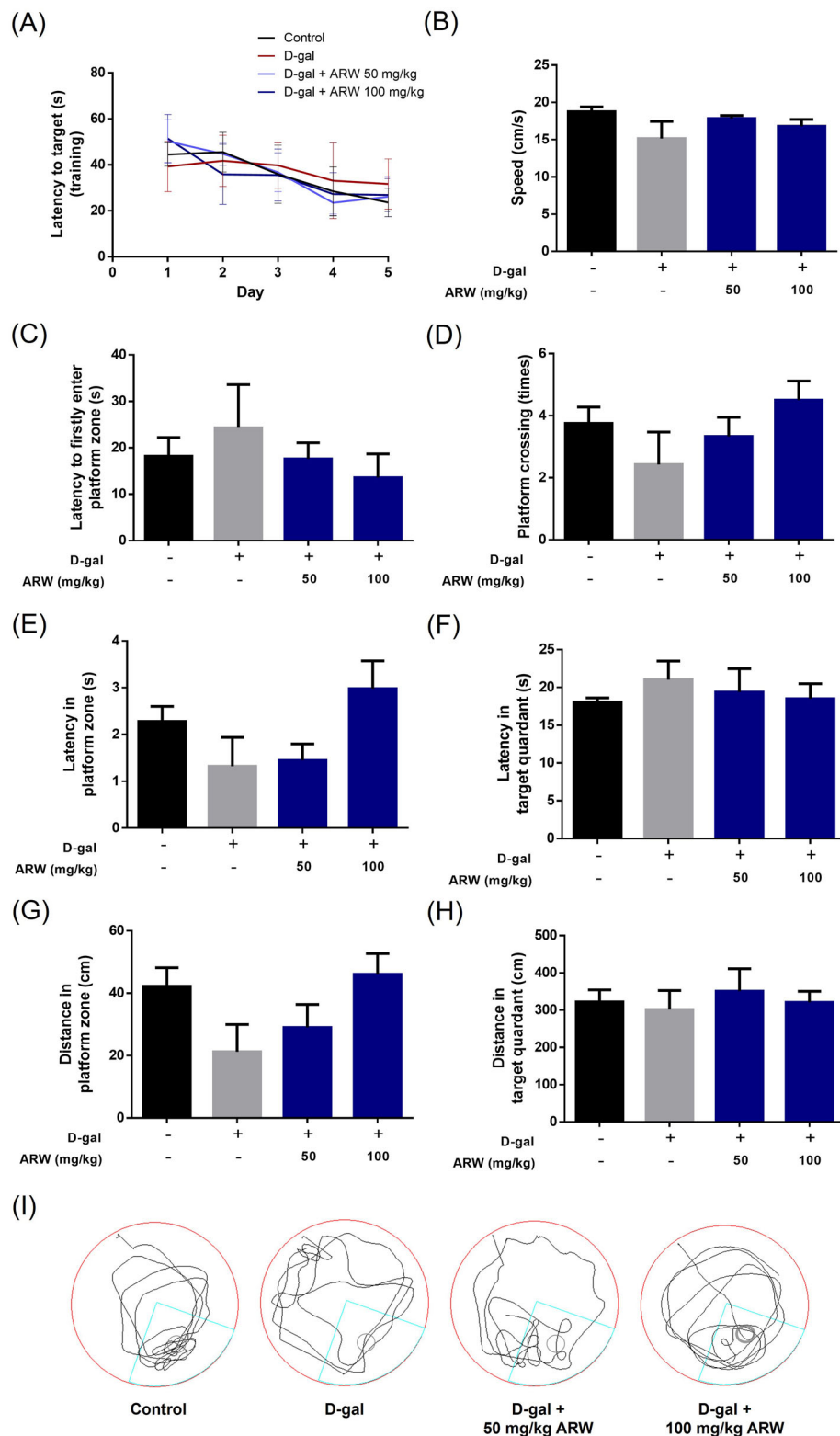
FIGURE 2 | **Effect of *Amauroderma rugosum* extract (ARW) treatment on memory and cognitive functions in D-galactose-induced aging mice**. The mice were treated with D-galactose for 12 weeks with different doses of the ARW. Mice that received no treatment were used as the control group. The Morris water maze test was performed after treatment. (A) Latency to target, (B) speed, (C) latency to first enter the platform zone, (D) number of platform crossings, (E) latency in the platform zone, (F) latency in the target quadrant, (G) distance traveled in the platform zone, and (H) distance in the target quadrant were measured for all experimental groups. (I) The moving trajectory of mice in each group. The gray circle indicates the platform zone, whereas the blue lines indicate the platform quadrant. Bars represent the mean ± standard deviation of 10 independent experiments.
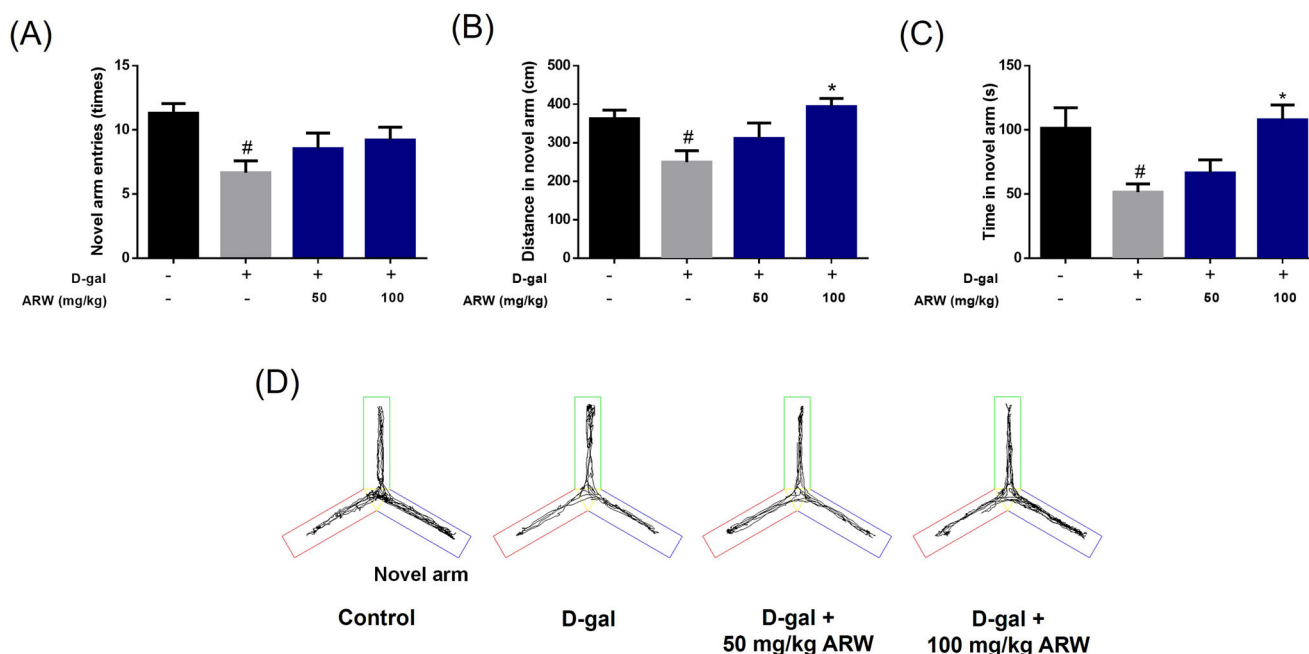
FIGURE 3 | Effect of *Amauroderma rugosum* extract (ARW) treatment on spatial reference memory in D-galactose-induced aging mice. The mice were treated with D-galactose for 12 weeks with different doses of ARW. Mice that received no treatment were used as the control group. The Y-maze test was conducted after treatment. (A) The number of novel arm entries, (B) distance traveled in the novel arm, and (C) time spent in the novel arm were measured. (D) The moving trajectories were recorded in all experimental groups. Bars represent the mean ± standard deviation of 10 independent experiments. #$p < 0.05$ indicates a statistically significant difference compared with the values of the control group. *$p < 0.05$ indicates a statistically significant difference compared with the values of the D-galactose-treated group.

were administered 100 mg/kg ARW. These findings suggest that ARW could improve spatial working memory, which requires interaction across several brain regions, such as the hippocampus and prefrontal cortex. There was no difference between the male and female mice (Figure S3).

3.5 | Effect of the ARW on Motor Skill Learning and Motor Coordination in Aging Mice

The results of the rotarod test showed that the amount of time the D-galactose-induced aging mice remained on the rotarod was shorter than that of the control group (Figure 4A). In addition, the D-galactose-induced aging mice fell more easily, even when the rotary speed was lower (Figure 4B). After treatment with 100 mg/mL ARW, the fall latency was longer (from 43.06 ± 11.61 to 58.24 ± 5.07 s; Figure 4A), and the mice could stay on the rotarod with a faster rotary speed (from 8.63 ± 1.56 to 11.60 ± 2.15 rpm; Figure 4B). These findings indicate that ARW can improve motor skill learning and coordination during aging. Moreover, there was no difference between the male and female mice (Figure S4).

## 3.6 | Effect of the ARW on Brain Nerves in the Hippocampus of Aging Mice

Karyopyknosis (irreversible condensation of chromatin in the nucleus of a cell undergoing necrosis or apoptosis) is a process that occurs prior to cell death. An increase in karyopyknosis is an indicator of neurodegenerative disease. Histological examination

showed that D-galactose-induced karyopyknosis mainly occurred in the dentate gyrus (Figure 5B) but not in the cornu ammonis 1 in the hippocampus (Figure 5C). The dentate gyrus is considered the "gateway" to the hippocampus and plays a crucial role in spatial memory formation. D-Galactose-induced karyopyknosis in the dentate gyrus was inhibited by the ARW in a dose-dependent manner (Figure 5B). In addition, as shown in Figure 5D, the brain neurons of the mice in the control group showed a rounded central vesicular nucleus with a prominent nucleolus. The cytoplasm contained prominent basophilic granules. However, in D-galactose-treated mice, the signs of neuronal injuries and histological changes were present. There were several hyperchromatic and pyknotic nuclei, along with a vacuolated cytoplasm. Signs of neuronal necrosis, also known as ghost cells, including neuronal cytoplasmic shrinkage, were also predominant. After treatment with 100 mg/mL ARW, the signs of neuronal injuries were reduced.

3.7 | Protective Effects on ARW and Its Ingredients Against D-Galactose-Treated SH-SY5Y Cells

The viability of the SH-SY5Y cells was decreased after exposure to 300 mM D-galactose. The ARW and its ingredients, including polysaccharides, ganoderic acid A, ganoderic acid D, ganoderic acid J, oleamide, GAE, uridine, and guanosine, inhibited the viability of the D-galactose-treated SH-SY5Y cells to varying degrees. When administered at 0.5 mg/mL, the ARW and ARP increased the proportion of viable D-galactose-treated cells
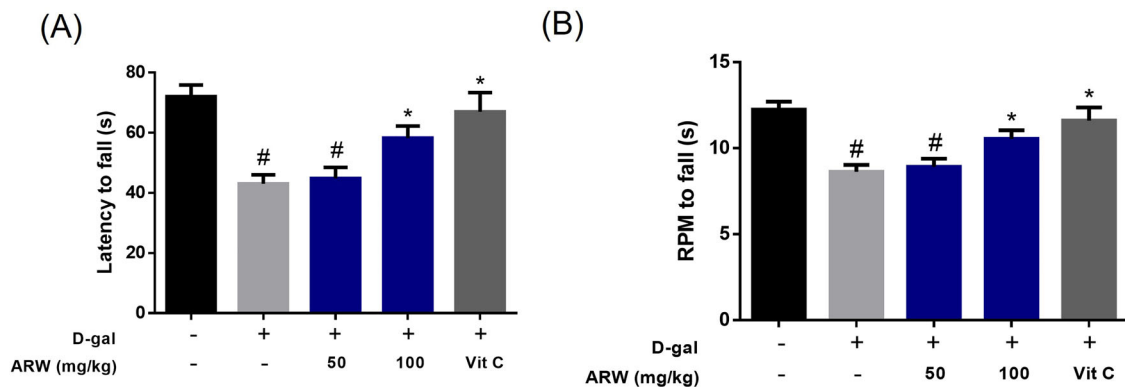
FIGURE 4 | **Effect of *Amauroderma rugosum* extract (ARW) treatment on motor skill learning and motor coordination in the D-galactose-induced aging mice**. The mice were treated with D-galactose for 12 weeks with different doses of ARW. Mice that received no treatment were used as the control group. The vitamin C-treated group was used for comparison. The rotarod test was performed after treatment. (A) Latency to fall and (B) speed required for the mice to fall (rotation per minute, RPM) were measured for all experimental groups. Bars represent the mean ± standard deviation of 10 independent experiments. #$p < 0.05$ indicates a statistically significant difference compared with the values of the control group. *$p < 0.05$ indicates a statistically significant difference compared with the values of the D-galactose-treated group.

from 47.86% to 65.85% and from 53.04% to 71.94%, respectively (Figure 6A,B). The application of GAE at concentrations below 10 μM had no effect. Still, concentrations exceeding 50 μM had a protective effect on the D-galactose-treated SH-SY5Y cells, resulting in a notable increase in cell viability from 49.72% to 70.93% at 50 μM (Figure 6C). Ganoderic acid J below 1 μM did not affect the cell viability, but 10 μM ganoderic acid J increased the amount of D-galactose-treated SH-SY5Y cells from 48.14% to 60.63% (Figure 6D). Ganoderic acid A, ganoderic acid D, oleamide, uridine, and guanosine did not affect the viability of D-galactose-treated SH-SY5Y cells even though 100 μM was used.

3.8 | Antioxidant Effects of the ARW and Its Ingredients on the D-Galactose-Treated SH-SY5Y Cells

The antioxidant properties of the ARW and ARP were investigated in the D-galactose-treated SH-SY5Y cells. Flow cytometry revealed a 3.9-fold increase in the ROS levels in the D-galactose-treated SH-SY5Y cells. However, applying D-galactose only resulted in a modest elevation in ROS levels, with an increase of 1.9- and 1.5-fold when the cells were pretreated with 2 mg/mL of ARW and ARP, respectively (Figure 6E,F). Gallic acid, guanosine, and uridine reduced intracellular and D-galactose-induced ROS levels by 23%, 26%, and 20%, respectively, when the concentration was higher than 100 μM; however, no effect was observed when the concentration was lower than 100 μM. Ganoderic acid A, ganoderic acid D, ganoderic acid J, and oleamide did not affect intracellular ROS levels even when 100 μM was used.

3.9 | Anti-Senescent and Antiapoptotic Effects of ARW and ARP on the D-Galactose-Treated SH-SY5Y Cells

The intracellular activity of β-galactosidase is a classic marker of cellular senescence. Therefore, β-galactosidase activity in

cells was detected using flow cytometry. The results revealed a 63.80% ± 6.41% increase in β-galactosidase activity in the D-galactose-treated SH-SY5Y cells. However, the increase in β-galactosidase activity was suppressed to 29.10% ± 9.91% and 14.51% ± 7.84% when the cells were pretreated with 2 mg/mL ARW and ARP, respectively, for 48 h (Figure 7A).

The antiapoptotic effects of the ARW on the SH-SY5Y cells were investigated using Annexin V-FITC/PI double labeling and flow cytometry. Treatment with 300 mM D-galactose increased the proportion of apoptotic cells from 18.70% ± 5.26% to 47.95% ± 7.99%; however, the proportion of apoptotic cells only increased to 27.15% ± 6.23% and 23.36% ± 7.92% when the D-galactose-treated cells were treated with 2 mg/mL ARW and ARP, respectively, for 48 h (Figure 7B).

3.10 | Effects of ARW and ARP on the Expression of the mTOR/Akt Protein and Pro/Antioxidant Enzyme Levels in the D-Galactose-Treated SH-SY5Y Cells

The mTOR/Akt-dependent signaling pathways play a significant role in modulating neuronal cell death. Treatment with 300 mM D-galactose substantially increased the protein expression ratios of phospho-mTOR/mTOR and phospho-Akt/Akt in the SH-SY5Y cells by 447% and 1175%, respectively (Figure 8B). The ratio of phospho-mTOR/mTOR decreased when the SH-SY5Y cells were pretreated with ARW and ARP. In contrast, the ratio of phospho-Akt/Akt was decreased by the ARW but was not significantly affected by the ARP (Figure 8C).

D-Galactose treatment did not significantly alter the protein expression of SOD-1, CAT, or HO-1. However, treatment with 2 mg/mL ARW or ARP enhanced the protein expression of SOD-1 from 24% to 26% (Figure 8E). Neither the ARW nor ARP altered the protein expression levels of CAT (Figure 8F). The ARW and ARP (2 mg/mL) increased HO-1 expression by 68% and 26%, respectively (Figure 8G).
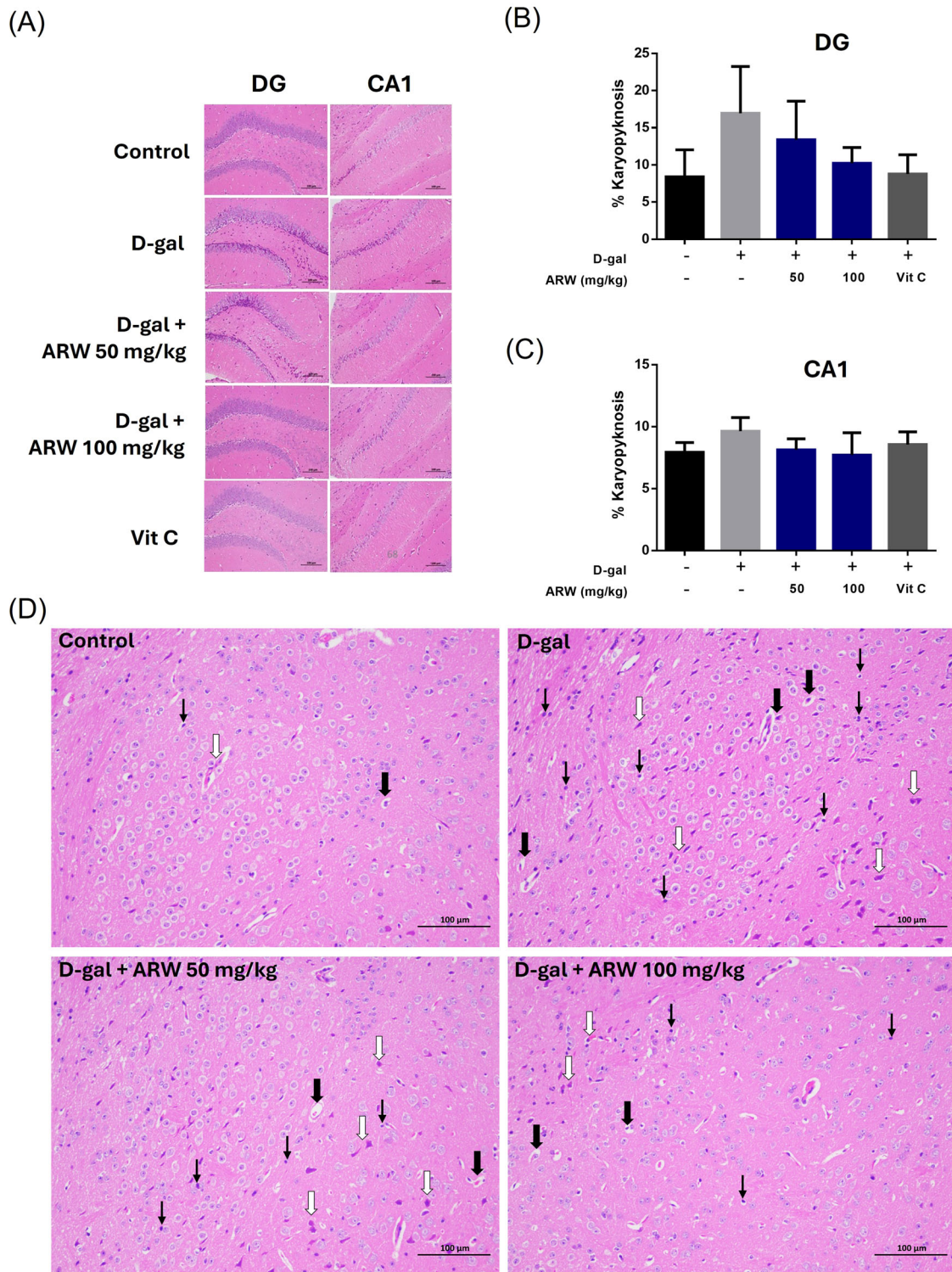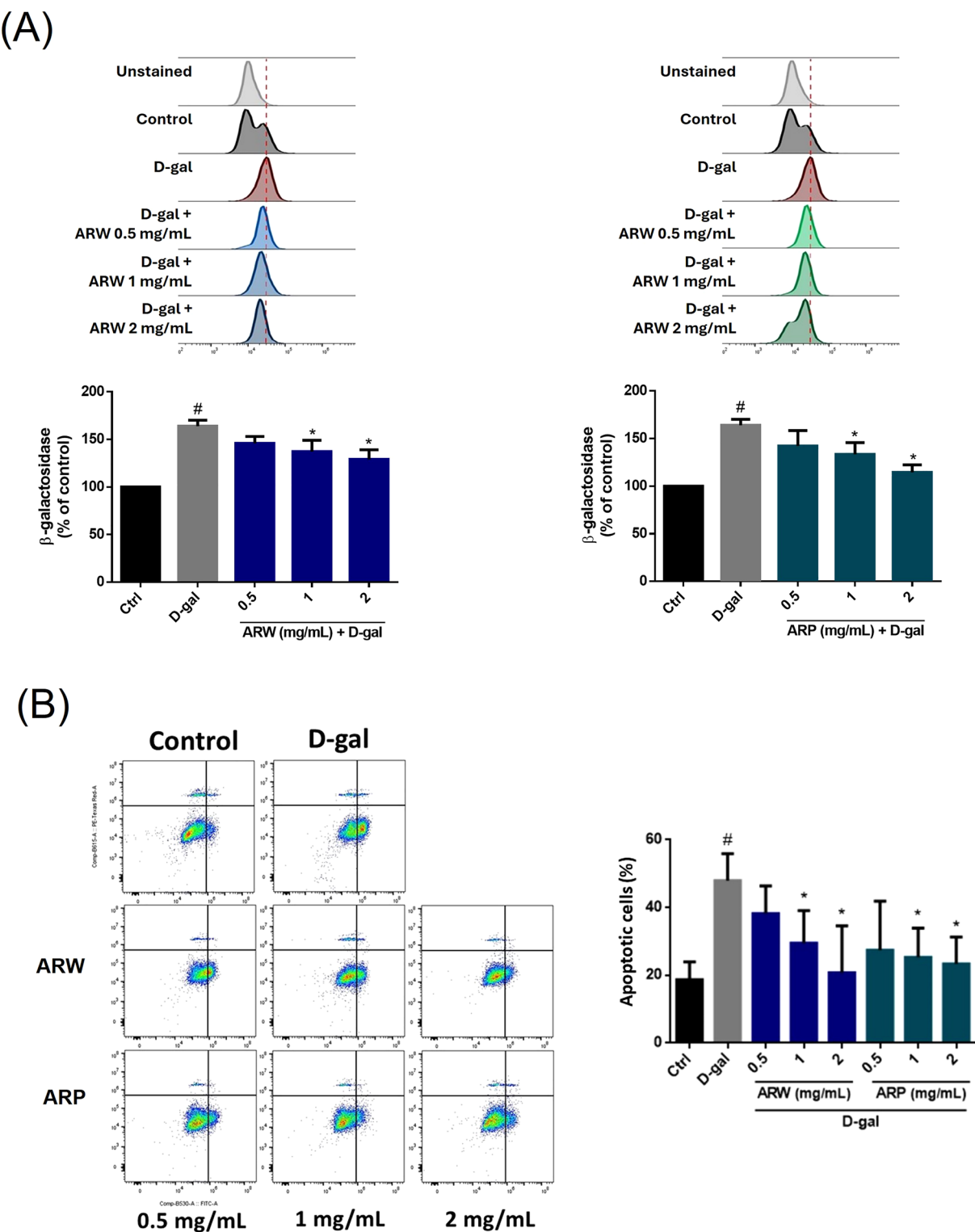
FIGURE 5 | **Effect of *Amauroderma rugosum* extract (ARW) on structural damage in the hippocampus of D-galactose-induced aging mice**. The mice were treated with D-galactose for 12 weeks with or without different doses of the ARW. Mice that received no treatment were used as the control group. The vitamin C treatment was used for comparison. Brain sections were stained with hematoxylin and eosin. (A) Images are presentative of 10 experiments. The percentages of karypyknosis in (B) dentate gyrus (DG) and (C) cornu ammonis (CA) 1 in the hippocampus were quantified. (D) Histological changes predominantly presented in D-galactose-treated groups, including pyknosis (thin arrow), vacuolated cells (thick arrow), and ghost cells (white arrow). The bar graphs represent the mean ± standard deviation of five independent experiments.
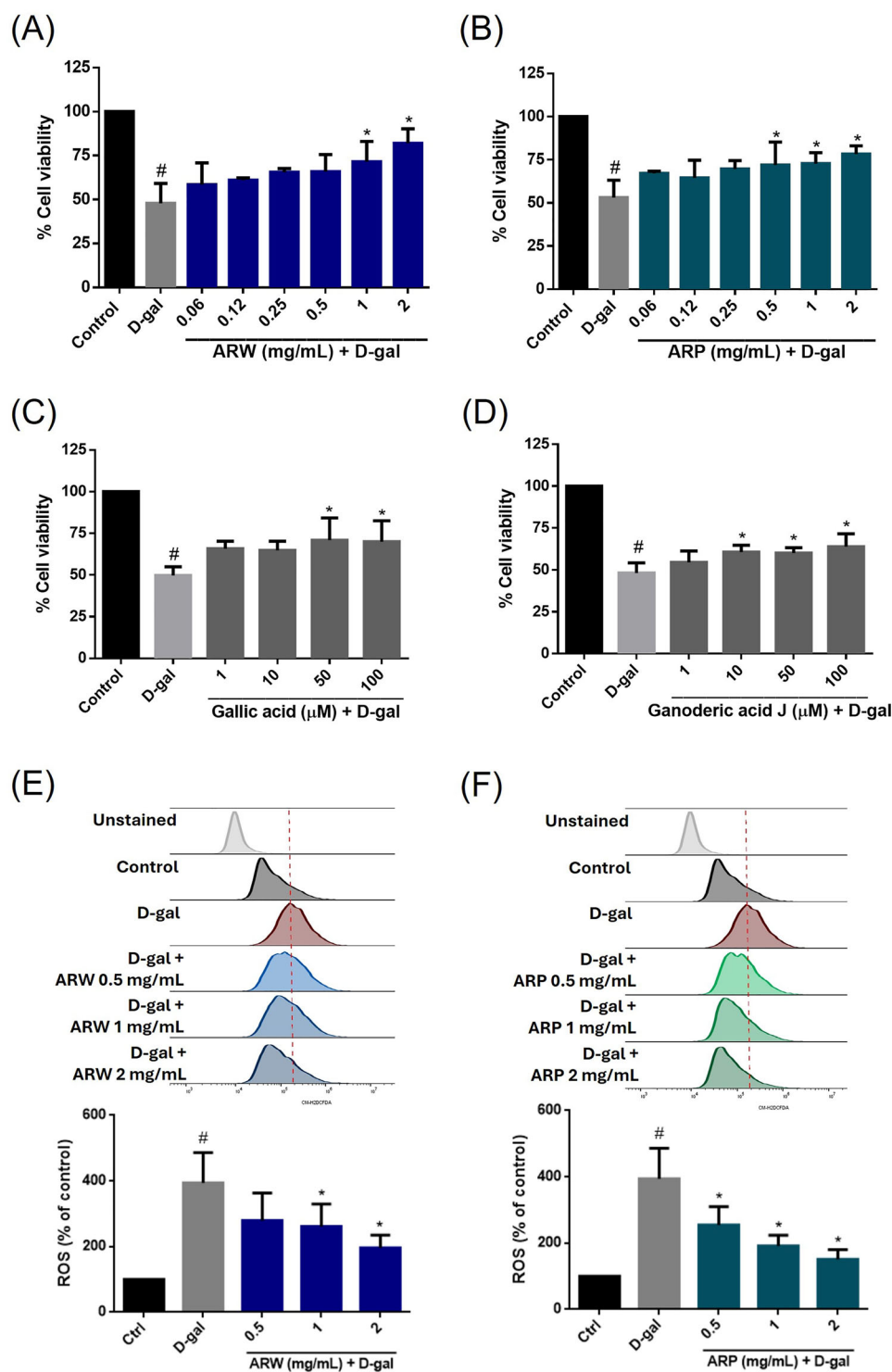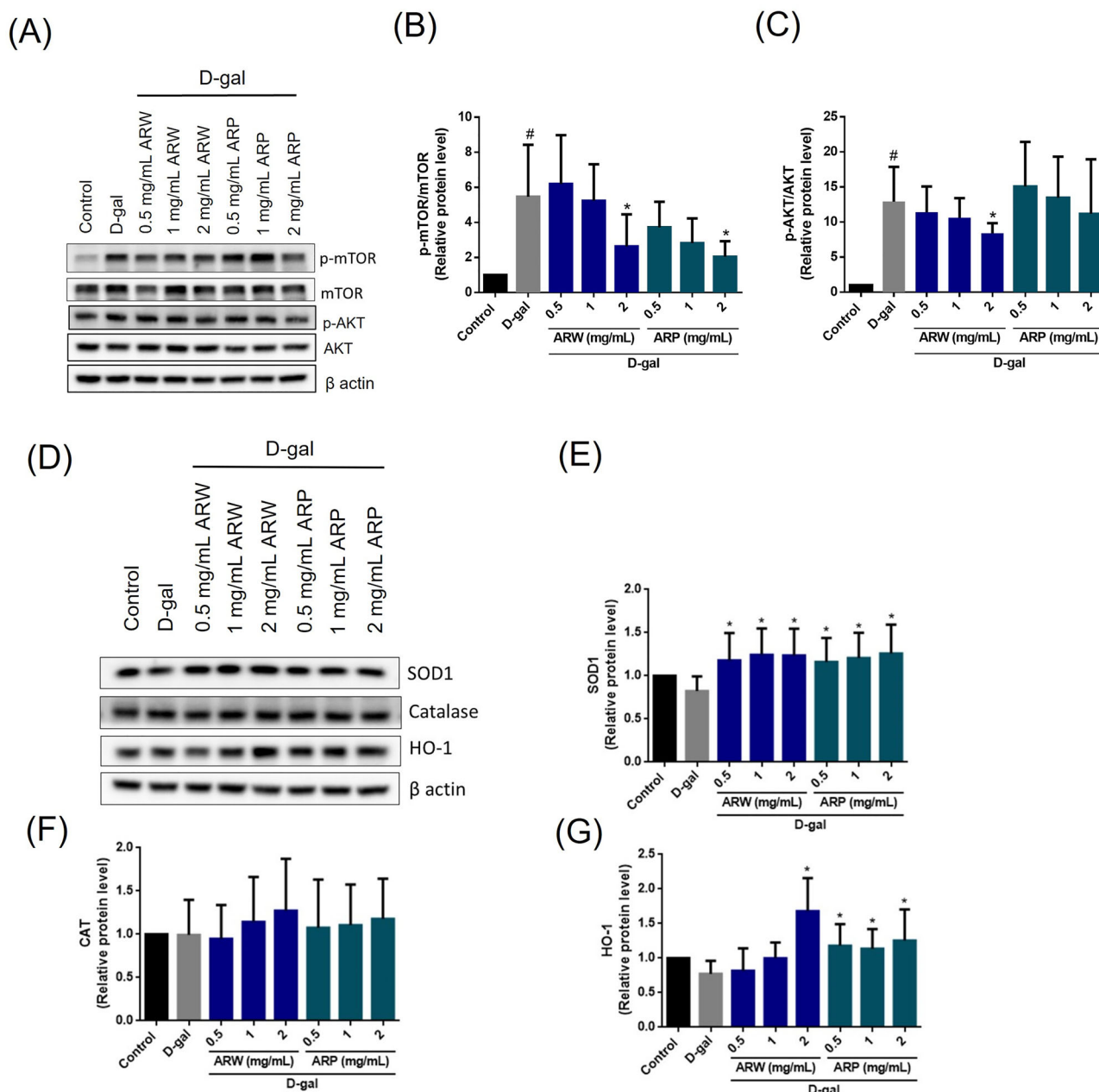
FIGURE 6 | **Effects of *Amauroderma rugosum* extract (ARW) and its constituents on viability and reactive oxygen species levels of D-galactose-induced SH-SY5Y cells**. SH-SY5Y cell viability was measured using the MTT assay. The cells were pre-incubated with different concentrations of (A) ARW, (B) ARP, (C) gallic acid, and (D) ganoderic acid J for 2 h, followed by treatment with 300 mM D-galactose for 24 h. Untreated cells served as controls. To measure the ROS, the SH-SY5Y cells were pretreated with different concentrations of (E) ARW and (F) ARP for 24 h and then treated with 300 mM D-galactose for 48 h. Untreated cells served as controls. The SH-SY5Y cells were subjected to CM-H$_2$DCFDA staining, and fluorescence signals were quantified using flow cytometry. Data are presented as percentages relative to the values of the control group (mean ± standard deviation of three independent experiments). #$p < 0.05$ indicates a statistically significant difference compared with the values of the control group. *$p < 0.05$ indicates a statistically significant difference compared with the values of the D-galactose-treated group. ARP, AR polysaccharide.

FIGURE 7 | **Effects of *Amauroderma rugosum* extract (ARW) and AR polysaccharide (ARP) on β-galactosidase activity and apoptosis in D-galactose-induced SH-SY5Y cells**. SH-SY5Y cells were pretreated with different concentrations of ARW and ARP for 2 h and then treated with 300 mM D-galactose for 24 h. Untreated cells served as controls. (A) β-Galactosidase activity and (B) apoptosis were detected by staining with Senescence Dye and Annexin V-FITC and P, respectively. The stained cells were quantified using flow cytometry. Data are presented as percentages relative to the control group values (mean $\pm$ standard deviation of three independent experiments). #$p < 0.05$ indicates a statistically significant difference compared with the values of the control group. *$p < 0.05$ indicates a statistically significant difference compared with the values of the D-galactose-treated group.

FIGURE 8 | **Effects of *Amauroderma rugosum* extract (ARW) and AR polysaccharide (ARP) treatment on TOR, Akt, and antioxidant enzyme protein levels in SH-SY5Y cells**. SH-SY5Y cells were treated with different concentrations of the ARW and ARP for 2 h and then treated with 300 mM D-galactose for 24 h. Untreated cells served as controls. (A) Protein expression levels of mTOR, p-mTOR, Akt, and p-Akt were determined by western blot analysis. The ratios of (B) p-mTOR/mTOR and (C) in ARW and ARP-treated groups were quantified. (D) Protein expression levels of SOD-1, CAT, and HO-1 in SH-SY5Y cells were determined by western blot analysis. The levels of (E) SOD-1, (F) CAT, and (G) HO-1 were quantified. Data are presented as the mean ± standard deviation of three independent experiments. #$p < 0.05$ indicates a statistically significant difference compared with the values of the control group. *$p < 0.05$ indicates a statistically significant difference compared with the values of the D-galactose-treated group.

3.11 | Significant Differences in Microbial Diversity After Treatment With ARW

No significant difference in α diversity was observed among the different groups, irrespective of sex, in terms of ACE, Chao1, Faith's PD, observed OTUs, Shannon, or Simpson indices (Figure 9A). The β diversity of different groups was significantly different in terms of Bray–Curtis, cosine, Hamming, and Jaccard distances ($p < 0.01$, PERMANOVA), which was demonstrated by the distinctive clustering in the principal coordinate analysis

(PCoA) biplot (Figure 9B). For the Firmicutes/Bacteroidetes ratio, a marginally significant difference was observed among the five groups (Figure 9C; $p = 0.0834$, Mann–Whitney U test).

A total of 1910 unique ASVs were identified, of which 51 were categorized as rare ASVs, with one count in the dataset (Figure 9E,F). After alignment, the ASVs were assigned to 21 phyla, 35 classes, 66 orders, 98 families, 171 genera, and 272 species. The most abundant phyla were Firmicutes and Bacteroidetes (Figure 9D).
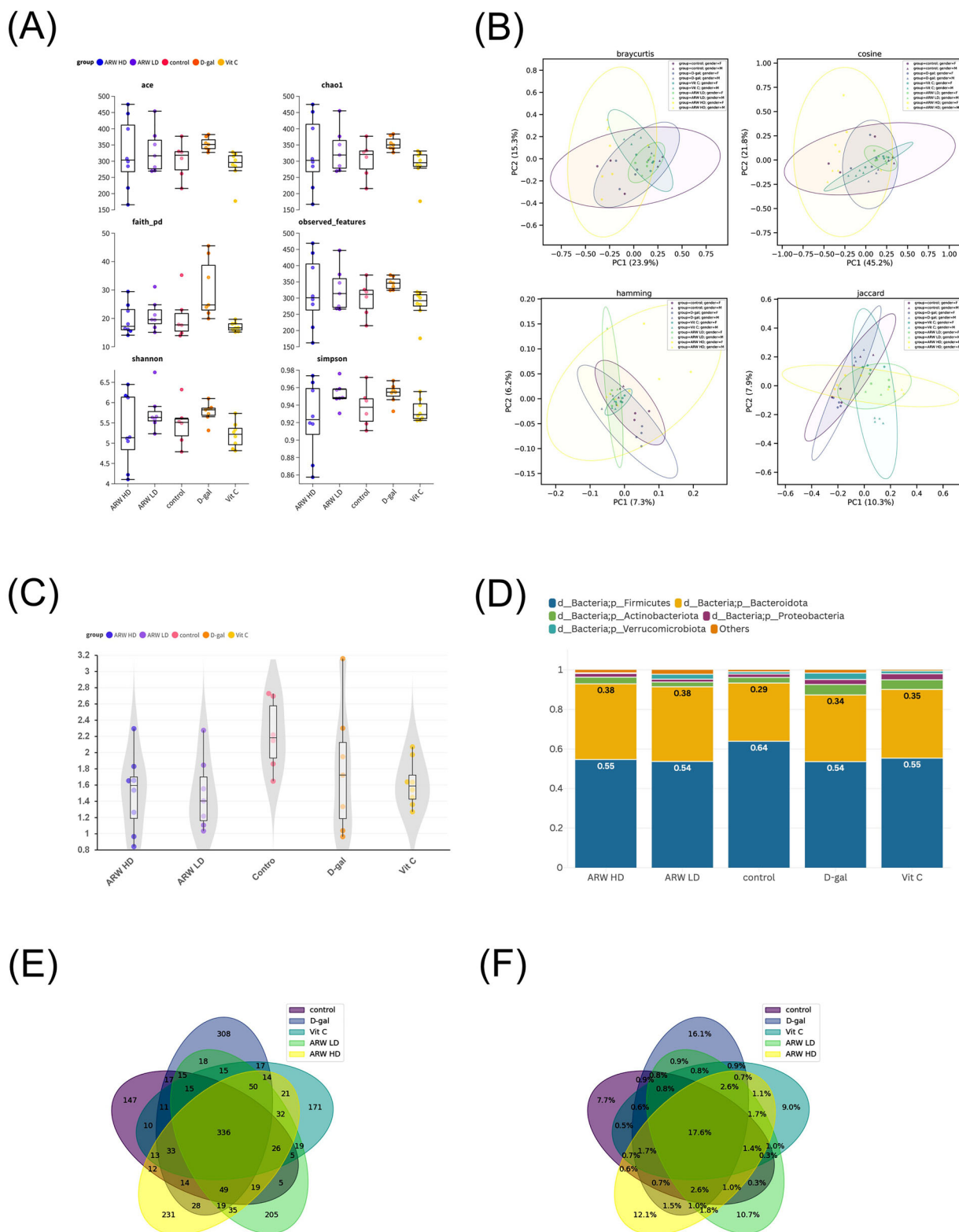
FIGURE 9 | **Effect of ARW on the intestinal flora in D-galactose-induced accelerated-aging mice**. The mice were treated with D-galactose with or without 50 mg/kg ARW (ARW LD), 100 mg/kg ARW (ARW HD), or 50 mg/kg vitamin C. (A) α Diversity in terms of ACE, Chao1, and Faith PD, observed OTUs, Shannon, and Simpson. (B) β-diversity analysis biplot based on Bray–Curtis, cosine, Hamming, and Jaccard distances (PERMANOVA, 999 permutations). (C) Boxplot of the Firmicutes/Bacteroidetes (F/B) ratio (Mann–Whitney U test). (D) Relative abundance of the dominant phyla (Firmicutes, Proteobacteria, Actinobacteria, Verrucomicrobiota, and Bacteroidetes) among different groups. (E) Venn diagram of all the ASVs among different groups. (F) Venn diagram of the ASVs (excluding rare ASVs) among different groups. ARW, *Amauroderma rugosum* extract.

3.12 | Effects of the ARW on Differential Abundance

Differential abundance at the ASV level was analyzed using ANCOM-BC. Ten ASVs were differentially expressed in the ARW-treated group ($p < 0.001$, Mann–Whitney U test) (Table 2). *Lactobacillus reuteri* was the most differentially abundant species, with 4.1- and 4.0-fold increases in the ARW-treated group than in the control and D-galactose-treated groups, respectively. A higher abundance of *Flavonifractor plautii*, *Muribaculum intestinale*, *Vampirovibrio chlorellavorus*, and an unidentified species in the *Clostridium* genus was also observed in the ARW-treated group, with at least a 2-fold increase compared with that in the control and D-galactose-treated groups. In contrast, the ARW-treated group had a lower relative abundance of *Clostridium scindens*, *Adlercreutzia caecimuris*, and *Kineothrix alysoides* than the control and D-galactose-treated groups. A high relative abundance of *Anaerobacterium chartisolvens* and *Paludihabitans psychrotolerans* was found in the D-galactose-treated group than in the control group. The D-galactose-induced increase in these bacteria was suppressed by ARW treatment.

4 | Discussion

Several empirical studies have indicated the potential effectiveness of dietary antioxidants in the prevention and treatment of neurodegenerative disorders (Andrade et al. 2019). An example is *G. lucidum*, a renowned edible and medicinal fungus in Asia. *G. lucidum* extract alleviates MPTP-induced parkinsonism and protects dopaminergic neurons from oxidative stress in mice (Ren et al. 2019). It also protects against mitochondrial dysfunction and death in hippocampal neurons in rodent models (Zhou et al. 2021). Similar to *G. Lucidum*, AR belongs to the Ganodermataceae family. Our previous research showed that ARW exhibits antioxidant and mitochondrial protective properties in 6-hydroxydopamine-treated PC12 and SH-SY5Y cells (Li et al. 2021; Rangsinth et al. 2024). Given that oxidation and mitochondrial dysfunction are significant indicators of aging, we investigated the neuroprotective effects of AR in a mouse model.

This study employed a D-galactose-induced aging mouse model rather than a naturally aging mouse model for two reasons. First, it enabled us to replicate aging-like effects in a shorter time. Second, D-galactose-induced aging mice exhibit a higher survival rate when compared with naturally aging mice during the experimental duration, which is advantageous for preserving uniform study conditions. A prior study has demonstrated that administering D-galactose injections could lead to brain aging in mice, which closely resembles the aging process observed in the human brain. This includes various effects such as mitochondrial dysfunction, heightened oxidative stress, reduced ATP production, apoptosis, neuronal degeneration, and cognitive impairments (Shwe et al. 2018). D-Galactose induces the activation of NF-κB, which, in turn, increases the expression of neuroinflammation markers, resulting in memory impairment (Daroi, Dhage, and Juvekar 2022). In addition to impairments in learning and memory, mice treated with D-galactose also display symptoms of depression and anxiety (Samad, Hafeez, and Imran 2022). Consistent with previous reports (Daroi, Dhage, and Juvekar 2022; Samad, Hafeez, and Imran 2022), our findings from the open field, Morris water maze, Y-maze, and rotarod tests indicated that D-galactose-induced aging mice exhibited cognitive dysfunction, memory decline, anxiety, and decreased locomotor capacity. The ARW effectively mitigated all the manifestations of aging. Neurodegeneration can be induced in the hippocampus, leading to cognitive dysfunction, which is closely associated with the pathological advancement of AD (Kadar et al. 1998). In this context, our histological study revealed that ARW decreased neuropathological damage in the hippocampus of aging mice brains, confirming the neuroprotective effect of ARW.

Our previous LC–MS analysis identified ganoderic acid A, ganoderic acid D, ganoderic acid J, oleamide, uridine, guanosine, and GAE in the ARW (Shiu et al. 2022). In this study, none of the compounds, except GAE, exhibited both antioxidant and protective properties in D-galactose-treated SH-SY5Y cells. Gallic acid is regarded as a promising candidate for treating various neurological disorders (Bhuia et al. 2023). Gallic acid increased the levels of total thiols and glutathione peroxidase while reducing malondialdehyde levels in the hippocampus and striatum in a rat model of Parkinson's disease (Mansouri et al. 2013). The administration of GAE to the APP/PS1 mouse model of cerebral amyloidosis effectively resolved behavioral impairments, improved cerebral amyloidosis, and decreased the abundance of β-amyloid (Mori et al. 2020). Furthermore, the administration of GAE protected the structural and functional integrity of the hippocampus in rats with AD (Hajipour et al. 2016). Although ganoderic acid J reduced the D-galactose-induced toxicity in the SH-SY5Y cells, the antioxidant effects were not significant. The only reported pharmacological effect of ganoderic acid J is its anti-inflammatory effect on BV2 microglial cells (Jiao et al. 2016). The neuroprotective effects of ARW on D-galactose-treated SH-SY5Y cells were observed at concentrations exceeding 0.5 mg/mL. The ARW (0.5 mg/mL) contains GAE at a concentration of only 3.5 μM (Shiu et al. 2022). The concentration of ganoderic acid J in AR is 4.08 μg/g (unpublished data); therefore, 0.5 mg/mL of ARW contains only 4 nM of ganoderic acid J. Similarly, although uridine and guanosine showed antioxidant effects on D-galactose-induced SH-SY5Y cells, the concentrations of guanosine and uridine in 0.5 mg/mL ARW were only 2.03 and 2.3 μM, respectively (Shiu et al. 2022). The low levels of GAE, ganoderic acid J, guanosine, and uridine in 0.5 mg/mL ARW were insufficient to decrease the mortality and ROS levels in D-galactose-induced SH-SY5Y cells. This suggests that they may not have substantially contributed to the neuroprotective effects of ARW.

Polysaccharides may protect the nervous system. For instance, polysaccharides obtained from *G. lucidum* can reduce the production of pro-inflammatory cytokines induced by lipopolysaccharides or β amyloids in microglia (Cai, Li, and Pei 2017). Furthermore, the neuroprotective advantages of *Poria cocos* polysaccharides have been observed in rats with AD. The observed effects are ascribed to its capacity to alleviate oxidative stress, apoptosis, and inflammation, as well as to inhibit the MAPK/NF-κB pathway (Zhou et al. 2021). To confirm the neuroprotective properties of the polysaccharides in ARW, we generated a polysaccharide-enriched ARP extract via ethanol precipitation. Our study showed that the ARP had a slightly higher antioxidant activity than the ARW. Furthermore, the ability of ARP to reduce viability, senescence, ROS levels, and apoptosis in D-galactose-treated SH-SY5Y cells was comparable to that of ARW. Notably, ARP

TABLE 2 | Differentially abundant amplicon sequence variants (ASVs) (taxonomic units assigned by a q2-feature-classifier) identified via ANCOM with bias correction (ANCOM-BC).

Feature ID	Taxon	Change compared with control group	Change compared with D-galactose-treated group
3fffad398d97cb7a0552d8d6dcefd12c	f__Lactobacillaceae; g__Lactobacillus; s__Lactobacillus_reuteri	Increased by 4.11-fold	Increased by 4.03-fold
41b2a97301262c39e7e62ca362ff4cd0	f__Oscillospiraceae; g__uncultured; s__Flavonifractor plautii	Increased bb 2.82-fold	Increased by 2.94-fold
c7743825cd83d66ef7d34f525b4e937b	f__Muribaculaceae; g__Muribaculaceae; s__ Muribaculum intestinale	Increased by 2.03-fold	Increased by 2.21-fold
8e107d174b548edd43e9e95649e29156	f__Gastranaerophilales; g__Gastranaerophilales; s_Vampirovibrio chlorellavorus	Increased by 2.40-fold	Increased by 2.62-fold
273fb933777dd9fe9d1accc234777be7	f__Clostridia_vadinBB60_group; g__Clostridia_vadinBB60_group; s__unidentified	Increased by 2.11-fold	Increased by 2.02-fold
476cd97e7f40664d9437a51af902b5a5	f__Lachnospiraceae; s__Clostridium scindens	Decreased by 2.53-fold	Decreased by 1.89-fold
cc7083620a1615635742a5589dc4b06	f__Eggerthellaceae; g__Enterorhabdus; s_Adlercreutzia caecimuris	Decreased by 1.78-fold	Decreased by 2.28-fold
31d7ca8d8dce0fafd9cf1108f0ae40ee	f__Lachnospiraceae; g__Lachnospiraceae_NK4A136_group; s__Kineothrix alysoides	Decreased by 2.90-fold	Decreased by 2.92-fold
cfd7c6dacd1e82a0a214f41aab4acb45	f__Clostridia_UCG-014; g__Clostridia_UCG-014; s__Anaerobacterium chartisolvens	No difference	Decreased by 1.88-fold
4dd4fa3cf3181582ed0ba8b423944bdc	f__Ruminococcaceae; g__Paludicola; s_Paludihabitans psychrotolerans	No difference	Decreased by 1.37-fold

treatment enhanced the expression of antioxidant enzymes SOD-1 and HO-1. This effect may also contribute to preserving redox homeostasis in aging brain microenvironments. Taken together, these results suggest that polysaccharides found in AR possess neuroprotective properties.

The application of plant-derived secondary metabolites to manage and/or treat various neuronal disorders via the PI3K/Akt/mTOR signaling pathway has been proposed as a promising strategy for neuroprotection (Fakhri et al. 2021). Abnormal activation of the Akt/mTOR pathway is linked to neurodegenerative disorders. Akt is recruited to the cell membrane after activating PI3K and phosphorylating phosphatidylinositol 4,5-bisphosphate (PIP2). Akt then phosphorylates GSK-3β, which plays a crucial role in neurodegenerative diseases. It also affects inflammatory mediators (ILs, COX, NF-κB), apoptotic pathways (e.g., Bax/Bcl-2, caspases), and oxidative factors (e.g., ROS, Nrf2, SOD-1, CAT, HO-1) in neurodegenerative disorders (Zarneshan et al. 2020). mTORC1, one of two complexes of mTOR, suppresses autophagy by phosphorylating and inhibiting key autophagy-related proteins like Atg13 and ULK1 (Vucicevic et al. 2020). Therefore, overactivity of mTOR may impair the autophagy process, leading to the accumulation of toxic protein aggregates like β-amyloid in AD and alpha-synuclein in Parkinson's disease. It has been reported that the AKT/mTOR signaling pathway is upregulated during natural aging (Zhong et al. 2024) and D-galactose-induced accelerated aging in mice (Chen et al. 2019). Phospho-mTOR protein expression is increased in D-galactose-induced senescent neuronal stem cells (Chen et al. 2018). Consistent with this finding, our study showed that D-galactose increased the expression of phospho-mTOR. This effect of D-galactose was attenuated by both ARW and ARP, suggesting that they may exert a neuroprotective effect through the inactivation of the mTOR-dependent pathway.

Polysaccharides are large molecules with a restricted ability to pass through the blood–brain barrier. This poses a potential hindrance to using polysaccharides for therapeutic purposes in brain disease. Additional studies are required to determine the optimal molecular size. The gut–brain axis has emerged as a prominent area of brain disease research over the past few decades. Aging significantly influences gut microbiota imbalance, leading to the proliferation of numerous bacteria that trigger inflammation, which contributes to the progression of neurodegenerative disorders (Giovannini et al. 2021). Recent research has indicated that polysaccharides can serve as prebiotics, potentially restoring the balance of the gut microbiota, thus providing benefits in alleviating neurodegenerative symptoms (Gao, Liang, and Liu 2024).

In view of that, the effect of ARW on the mouse microbiome was assessed. Owing to the small sample size, this analysis was primarily exploratory. However, the ARW affected the composition of the intestinal flora, which may introduce a novel field of investigation in the study of aging. For instance, *L. reuteri* was more prevalent in ARW-treated mice. Administration of *L. reuteri* can mitigate the activation of pro-inflammatory signaling pathways, endoplasmic reticulum stress, and autophagy in the hippocampus of rats fed a high-fat and fructose diet (Mazzoli et al. 2024). *L. reuteri* also mitigates the detrimental effects of diabetes on the hippocampus (Lin et al. 2023). Administration of a symbiotic supplement containing *Corni fructus* and *L. reuteri* led to significant enhancement in cognitive function in mice with DSS-induced behavioral disorders (Lee et al. 2022). An increase in *L. reuteri* in the intestine may contribute to the neuroprotective effects of ARW. The molecular mechanism of neuroprotective action of *L. reuteri* may be multifaceted. First, *L. reuteri* is capable of synthesizing neurotransmitters such as GABA and serotonin, which play critical roles in mood regulation, cognition, and neural communication (Yong et al. 2020). It is not implausible that *L. reuteri* may produce substances to reduce chronic neuroinflammation, which is a hallmark of many neurodegenerative diseases, including AD and Parkinson's diseases. For instance, lipoteichoic acid derived from *L. reuteri* can exert anti-inflammatory effects by promoting anti-inflammatory cytokines like IL-10 while reducing pro-inflammatory cytokines like IL-6 and TNF-alpha (Lu et al. 2022). In addition, *L. reuteri* produces metabolites such as short-chain fatty acids, including butyrate, propionate, and acetate, which are capable of histone deacetylase inhibition (Arpaia et al. 2013; Luu et al. 2019). Inhibition of histone deacetylase may increase the acetylation of genes and influence gene transcription related to neuroprotection. Furthermore, short-chain fatty acids maintain gut barrier integrity by increasing the expression of tight junction proteins (Huang et al. 2024). A stronger gut barrier can prevent the infiltration of pro-inflammatory molecules and pathogens into the brain, thus protecting against neurodegenerative damage.

C. scindens is also a bacterium that may be related to neurodegeneration. According to previous reports, consumption of polysorbate 80, a commonly used substance that helps mix ingredients in food and medicine, can lead to an increase of *C. scindens* in the gut and worsen the decline in cognitive function in senescence-accelerated mice (Zhang et al. 2024). This bacterium metabolizes cholic acid to deoxycholic acid, which is a secondary bile acid. Recent research has indicated a connection between bile acid metabolism disorders and central nervous system diseases (Grant and DeMorrow 2020). Multiple studies have demonstrated that bile acid metabolism can affect learning, memory, and cognitive functions (Liu et al. 2024). At the molecular level, secondary bile acids may interact with various receptors in the brain, such as farnesoid X receptors, leading to neuroinflammatory responses and triggering signaling cascades that can damage neural cells (Sabahat et al. 2024; McMillin et al. 2016). Owing to the harmful effects of secondary bile acids on brain function, it is speculated that the reduced presence of *C. scindens* may be beneficial in preventing neurodegenerative diseases.

As a natural product, AR has numerous advantages. It is easily cultivated, and thus, its production cost is relatively low. The standard dosage of AR in traditional Chinese medicine is 10–15 g per decoction (Zheng, Cheung, and Leung 2022). The long-term medical and dietary records did not report any adverse effects or toxicities associated with its consumption. Furthermore, a study conducted on live Sprague–Dawley rats found that even with a dose of 2 g/kg of AR mycelial powder, there were no changes in body weight or pathological changes in various organs (Fung et al. 2017). Moreover, the viability of PC-12 and SH-SY5Y cells, as well as the lifespan of *C. elegans*, remained unaffected when exposed to 2 mg/mL ARW (Li et al. 2021; Rangsinth et al. 2024). Therefore, AR is considered safe.

5 | Conclusions

This study provides the first evidence that the ARW protects hippocampal neurons, leading to enhanced learning, memory, and locomotor abilities in ᴅ-galactose-induced aging in mice. In addition, the ARW protects neuronal cells by reducing oxidative stress and apoptosis. The molecular mechanisms are likely mediated through the mTOR-dependent signaling pathway and the upregulation of the antioxidant enzymes SOD-1 and HO-1. The neuroprotective effects of the ARW are primarily attributed to the presence of polysaccharides as the main active ingredient. The ARW also alters the microbial diversity in the intestine, which may contribute to its neuroprotective effect through the microbial–gut–brain axis. These findings suggest that AR has the potential to be used as a beneficial food and medicine for the prevention and treatment of age-related neurodegenerative diseases.

Conflicts of Interest

The authors declare no conflicts of interest.

References

Andrade, S., M. J. Ramalho, J. A. Loureiro, and M. D. C. Pereira. 2019. "Natural Compounds for Alzheimer's Disease Therapy: A Systematic Review of Preclinical and Clinical Studies." *International Journal of Molecular Sciences* 20, no. 9: 2313. https://doi.org/10.3390/ijms20092313.

Arpaia, N., C. Campbell, X. Fan, et al. 2013. "Metabolites Produced by Commensal Bacteria Promote Peripheral Regulatory T-Cell Generation." *Nature* 504: 451–455. https://doi.org/10.1038/nature12726.

Bhuia, M. S., M. M. Rahaman, T. Islam, et al. 2023. "Neurobiological Effects of Gallic Acid: Current Perspectives." *Chinese Medicine* 18, no. 1: 27. https://doi.org/10.1186/s13020-023-00735-7.

Cai, Q., Y. Li, and G. Pei. 2017. "Polysaccharides From *Ganoderma lucidum* Attenuate Microglia-Mediated Neuroinflammation and Modulate Microglial Phagocytosis and Behavioural Response." *Journal of Neuroinflammation* 14, no. 1: 63. https://doi.org/10.1186/s12974-017-0839-0.

Chen, L., H. Yao, X. Chen, et al. 2018. "Ginsenoside Rg1 Decreases Oxidative Stress and Down-Regulates Akt/mTOR Signalling to Attenuate Cognitive Impairment in Mice and Senescence of Neural Stem Cells Induced by D-Galactose." *Neurochemical Research* 43, no. 2: 430–440. https://doi.org/10.1007/s11064-017-2438-y.

Chen, P., F. Chen, J. Lei, Q. Li, and B. Zhou. 2019. "Activation of the miR-34a-Mediated SIRT1/mTOR Signaling Pathway by Urolithin A Attenuates D-Galactose-Induced Brain Aging in Mice." *Neurotherapeutics* 16, no. 4: 1269–1282. https://doi.org/10.1007/s13311-019-00753-0.

Daroi, P. A., S. N. Dhage, and A. R. Juvekar. 2022. "p-Coumaric Acid Protects Against D-Galactose Induced Neurotoxicity by Attenuating Neuroinflammation and Apoptosis in Mice Brain." *Metabolic Brain Disease* 37, no. 7: 2569–2579. https://doi.org/10.1007/s11011-022-01007-3.

Fakhri, S., A. Iranpanah, M. M. Gravandi, et al. 2021. "Natural Products Attenuate PI3K/Akt/mTOR Signaling Pathway: A Promising Strategy in Regulating Neurodegeneration." *Phytomedicine* 91: 153664. https://doi.org/10.1016/j.phymed.2021.153664.

Fung, S. Y., N. H. Tan, B. H. Kong, S. S. Lee, Y. S. Tan, and V. Sabaratnam. 2017. "Acute Toxicity Study and the In Vitro Cytotoxicity of a Black Lingzhi Medicinal Mushroom, *Amauroderma rugosum* (Agaricomycetes), From Malaysia." *International Journal of Medicinal Mushrooms* 19, no. 12: 1093–1099. https://doi.org/10.1615/IntJMedMushrooms.2017024550.

Gao, J., Y. Liang, and P. Liu. 2024. "Along the Microbiota-Gut-Brain Axis: Use of Plant Polysaccharides to Improve Mental Disorders." *International Journal of Biological Macromolecules* 265, no. 2: 130903. https://doi.org/10.1016/j.ijbiomac.2024.130903.

Giovannini, M. G., D. Lana, C. Traini, and M. G. Vannucchi. 2021. "The Microbiota–Gut–Brain Axis and Alzheimer Disease. From Dysbiosis to Neurodegeneration: Focus on the Central Nervous System Glial Cells." *Journal of Clinical Medicine* 10, no. 11: 2358. https://doi.org/10.3390/jcm10112358.

Goldsteins, G., V. Hakosalo, M. Jaronen, M. H. Keuters, Š. Lehtonen, and J. Koistinaho. 2022. "CNS Redox Homeostasis and Dysfunction in Neurodegenerative Diseases." *Antioxidants* 11, no. 2: 405. https://doi.org/10.3390/antiox11020405.

Grant, S. M., and S. DeMorrow. 2020. "Bile Acid Signaling in Neurodegenerative and Neurological Disorders." *International Journal of Molecular Sciences* 21, no. 17: 5982. https://doi.org/10.3390/ijms21175982.

Hajipour, S., A. Sarkaki, Y. Farbood, A. Eidi, P. Mortazavi, and Z. Valizadeh. 2016. "Effect of Gallic Acid on Dementia Type of Alzheimer Disease in Rats: Electrophysiological and Histological Studies." *Basic and Clinical Neuroscience* 7, no. 2: 97–106. https://doi.org/10.15412/J.BCN.03070203.

Huang, Y., J. Hu, Q. Xia, et al. 2024. "Amelioration of Obesity and Inflammation by Polysaccharide From Unripe Fruits of Raspberry via Gut Microbiota Regulation." *International Journal of Biological Macromolecules* 261, no. pt. 2: 129825. https://doi.org/10.1016/j.ijbiomac.2024.129825.

Jiao, Y., T. Xie, L. H. Zou, Q. Wei, L. Qiu, and L. X. Chen. 2016. "Lanostane Triterpenoids From *Ganoderma curtisii* and Their NO Production Inhibitory Activities of LPS-Induced Microglia." *Bioorganic and Medicinal Chemistry Letters* 26, no. 15: 3556–3561. https://doi.org/10.1016/j.bmcl.2016.06.023.

Kadar, T., S. Dachir, B. Shukitt-Hale, and A. Levy. 1998. "Sub-Regional Hippocampal Vulnerability in Various Animal Models Leading to Cognitive Dysfunction." *Journal of Neural Transmission* 105, no. 8–9: 987–1004. https://doi.org/10.1007/s007020050107.

Kose, E., T. Yamamoto, N. Tate, A. Ando, H. Enomoto, and N. Yasuno. 2023. "Adverse Drug Event Profile Associated With Anti-Dementia Drugs: Analysis of a Spontaneous Reporting Database." *Die Pharmazie* 78, no. 5: 42–46. https://doi.org/10.1691/ph.2023.2584.

Kwong, T. C., E. C. T. Chau, M. C. H. Mak, et al. 2023. "Characterization of the Gut Microbiome in Healthy Dogs and Dogs With Diabetes Mellitus." *Animals (Basel)* 13, no. 15: 2479. https://doi.org/10.3390/ani13152479.

Lee, H. L., J. M. Kim, J. H. Moon, et al. 2022. "Anti-Amnesic Effect of Synbiotic Supplementation Containing *Corni fructus* and *Limosilactobacillus reuteri* in DSS-Induced Colitis Mice." *International Journal of Molecular Sciences* 24, no. 1: 90. https://doi.org/10.3390/ijms24010090.

Li, J., R. Li, X. Wu, et al. 2021. "*Amauroderma rugosum* Protects PC12 Cells Against 6-OHDA-Induced Neurotoxicity Through Antioxidant and Antiapoptotic Effects." *Oxidative Medicine and Cellular Longevity* 2021: 6683270. https://doi.org/10.1155/2021/6683270.

Lin, B., D. Xu, S. Wu, et al. 2021. "Antioxidant Effects of *Sophora davidii* (Franch.) Skeels on D-Galactose-Induced Aging Model in Mice via Activating the SIRT1/p53 Pathway." *Frontiers in Pharmacology* 12: 754554. https://doi.org/10.3389/fphar.2021.754554.

Lin, J. Y., B. C. K. Tsai, H. C. Kao, et al. 2023. "Neuroprotective Effects of Probiotic *Lactobacillus reuteri* GMNL-263 in the Hippocampus of Streptozotocin-Induced Diabetic Rats." *Probiotics and Antimicrobial Proteins* 15, no. 5: 1287–1297. https://doi.org/10.1007/s12602-022-09982-w.

Liu, A., Y. Li, L. Li, et al. 2024. "Bile Acid Metabolism Is Altered in Learning and Memory Impairment Induced by Chronic Lead Exposure." *Journal of Hazardous Materials* 471: 134360. https://doi.org/10.1016/j.jhazmat.2024.134360.

Lu, Q., Y. Guo, G. Yang, et al. 2022. "Structure and Anti-Inflammation Potential of Lipoteichoic Acids Isolated From Lactobacillus Strains." *Foods* 11, no. 11: 1610. https://doi.org/10.3390/foods11111610.

Luu, M., S. Pautz, V. Kohl, et al. 2019. "The Short-Chain Fatty Acid Pentanoate Suppresses Autoimmunity by Modulating the Metabolic-Epigenetic Crosstalk in Lymphocytes." *Nature Communications* 10: 760. https://doi.org/10.1038/s41467-019-08711-2.

Mani, S., R. Dubey, I. C. Lai, et al. 2023. "Oxidative Stress and Natural Antioxidants: Back and Forth in the Neurological Mechanisms of Alzheimer's Disease." *Journal of Alzheimer's Disease* 96, no. 3: 877–912. https://doi.org/10.3233/JAD-220700.

Mansouri, M. T., Y. Farbood, M. J. Sameri, A. Sarkaki, B. Naghizadeh, and M. Rafeirad. 2013. "Neuroprotective Effects of Oral Gallic Acid Against Oxidative Stress Induced by 6-Hydroxydopamine in Rats." *Food Chemistry* 138, no. 2–3: 1028–1033. https://doi.org/10.1016/j.foodchem.2012.11.022.

Mazzoli, A., M. S. Spagnuolo, F. De Palma, et al. 2024. "*Limosilactobacillus reuteri* DSM 17938 Relieves Inflammation, Endoplasmic Reticulum Stress, and Autophagy in Hippocampus of Western Diet-Fed Rats by Modulation of Systemic Inflammation." *Biofactors* 50, no. 6: 1236–1250. https://doi.org/10.1002/biof.2082.

McMillin, M., G. Frampton, M. Quinn, et al. 2016. "Bile Acid Signaling Is Involved in the Neurological Decline in a Murine Model of Acute Liver Failure." *American Journal of Pathology* 186, no. 2: 312–323. https://doi.org/10.1016/j.ajpath.2015.10.005.

Mori, T., N. Koyama, T. Yokoo, et al. 2020. "Gallic Acid Is a Dual *α*/*β*-Secretase Modulator That Reverses Cognitive Impairment and Remediates Pathology in Alzheimer Mice." *Journal of Biological Chemistry* 295, no. 48: 16251–16266. https://doi.org/10.1074/jbc.RA119.012330.

Nam, S. M., M. Seo, J. S. Seo, et al. 2019. "Ascorbic Acid Mitigates D-Galactose-Induced Brain Aging by Increasing Hippocampal Neurogenesis and Improving Memory Function." *Nutrients* 11, no. 1: 176. https://doi.org/10.3390/nu11010176.

Rangsinth, P., N. Pattarachotanant, W. Wang, et al. 2024. "Neuroprotective Effects of Polysaccharides and Gallic Acid From *Amauroderma rugosum* Against 6-OHDA-Induced Toxicity in SH-SY5Y Cells." *Molecules (Basel, Switzerland)* 29, no. 5: 953. https://doi.org/10.3390/molecules29050953.

Ren, Z. L., C. D. Wang, T. Wang, et al. 2019. "*Ganoderma lucidum* Extract Ameliorates MPTP-Induced Parkinsonism and Protects Dopaminergic Neurons From Oxidative Stress via Regulating Mitochondrial Function, Autophagy, and Apoptosis." *Acta Pharmacologica Sinica* 40, no. 4: 441–450. https://doi.org/10.1038/s41401-018-0077-8.

Reshma, B. S., T. Aavula, V. Narasimman, S. Ramachandran, M. M. Essa, and M. W. Qoronfleh. 2022. "Antioxidant and Antiaging Properties of Agar Obtained From Brown Seaweed *Laminaria digitata* (Hudson) in D-Galactose-Induced Swiss Albino Mice." *Evidence Based Complementary and Alternative Medicine* 2022: 7736378. https://doi.org/10.1155/2022/7736378.

Sabahat, S. E., M. Saqib, M. Talib, T. G. Shaikh, T. Khan, and S. J. Kailash. 2024. "Bile Acid Modulation by Gut Microbiota: A Bridge to Understanding Cognitive Health." *Annals of Medicine and Surgery (London)* 86, no. 9: 5410–5415. https://doi.org/10.1097/MS9.0000000000002433.

Samad, N., F. Hafeez, and I. Imran. 2022. "D-Galactose Induced Dysfunction in Mice Hippocampus and the Possible Antioxidant and Neuromodulatory Effects of Selenium." *Environmental Science and Pollution Research International* 29, no. 4: 5718–5735. https://doi.org/10.1007/s11356-021-16048-x.

Shiu, P. H. T., J. Li, C. Zheng, et al. 2022. "*Amauroderma rugosum* Extract Suppresses Inflammatory Responses in Tumor Necrosis Factor Alpha/Interferon Gamma-Induced HaCaT Keratinocytes." *Molecules (Basel, Switzerland)* 27, no. 19: 6533. https://doi.org/10.3390/molecules27196533.

Shwe, T., W. Pratchayasakul, N. Chattipakorn, and S. C. Chattipakorn. 2018. "Role of D-Galactose-Induced Brain Aging and Its Potential Used for Therapeutic Interventions." *Experimental Gerontology* 101: 13–36. https://doi.org/10.1016/j.exger.2017.10.029.

Vucicevic, L., M. Misirkic, D. Ciric, et al. 2020. "Transcriptional Block of AMPK-Induced Autophagy Promotes Glutamate Excitotoxicity in Nutrient-Deprived SH-SY5Y Neuroblastoma Cells." *Cellular and Molecular Life Sciences* 77, no. 17: 3383–3399.

Xiao, Z. T., M. Liu, and H. Q. He. 2017. "Domestication and Antioxidant Activities of *Amauroderma rugosum*." *Mycosystema* 36, no. 3: 358–366. https://doi.org/10.13346/j.mycosystema.160029.

Yong, S. J., T. Tong, J. Chew, and W. L. Lim. 2020. "Antidepressive Mechanisms of Probiotics and Their Therapeutic Potential." *Frontiers in Neuroscience* 13: 1361. https://doi.org/10.3389/fnins.2019.01361.

Zarneshan, S. N., S. Fakhri, M. H. Farzaei, H. Khan, and L. Saso. 2020. "Astaxanthin targets PI3K/Akt signaling pathway toward potential therapeutic applications." *Food and Chemical Toxicology* 145: 111714. https://doi.org/10.1016/j.fct.2020.111714.

Zhang, L., Z. Yin, X. Liu, et al. 2024. "Dietary Emulsifier Polysorbate 80 Exposure Accelerates Age-Related Cognitive Decline." *Brain, Behavior, and Immunity* 119: 171–187. https://doi.org/10.1016/j.bbi.2024.03.052.

Zheng, C. W., T. M. Y. Cheung, and G. P. H. Leung. 2022. "A Review of the Phytochemical and Pharmacological Properties of *Amauroderma rugosum*." *Kaohsiung Journal of Medical Sciences* 38, no. 6: 509–516. https://doi.org/10.1002/kjm2.12554.

Zhong, W., J. Chen, Y. He, L. Xiao, and C. Yuan. 2024. "The Polysaccharides From Balanophora Polyandra Enhanced Neuronal Autophagy to Ameliorate Brain Function Decline in Natural Aging Mice Through the PI3K/AKT/mTOR Signaling Pathway." *Neuroreport* 35, no. 8: 509–517. https://doi.org/10.1097/WNR.0000000000002024.

Zhou, X., Y. Zhang, Y. Jiang, C. Zhou, and Y. Ling. 2021. "*Poria cocos* Polysaccharide Attenuates Damage of Nervus in Alzheimer's Disease Rat Model Induced by D-Galactose and Aluminum Trichloride." *Neuroreport* 32, no. 8: 727–737. https://doi.org/10.1097/WNR.0000000000001648.

Supporting Information

Additional supporting information can be found online in the Supporting Information section.